

WIDEBAND MIMO ANTENNA
DEVELOPMENT FOR WIRELESS
COMMUNICATION

ABDUL WAFIY BIN KASSIM

Bachelor of Engineering Technology In (Electrical)
With Hons

UNIVERSITI MALAYSIA PAHANG

UNIVERSITI MALAYSIA PAHANG

DECLARATION OF THESIS AND COPYRIGHT

Author's Full Name : **ABDUL WAFIY BIN KASSIM**
Date of Birth :
Title : **WIDEBAND MIMO ANTENNA
DEVELOPMENT FOR WIRELESS
COMMUNICATION**
Academic Session : **2020/2021**

I declare that this thesis is classified as:

- CONFIDENTIAL** (Contains confidential information under the Official Secret Act 1997) *
- RESTRICTED** (Contains restricted information as specified by the organization where research was done)*
- OPEN ACCESS** I agree that my thesis to be published as online open access (Full Text)

I acknowledge that Universiti Malaysia Pahang reserves the following rights:

1. The Thesis is the Property of Universiti Malaysia Pahang
2. The Library of Universiti Malaysia Pahang has the right to make copies of the thesis for the purpose of research only.
3. The Library has the right to make copies of the thesis for academic exchange.

Certified by:

(Student's Signature)

(Supervisor's Signature)

New IC/Passport Number
Date: 5 FEBRUARY 2021

DR. MOHAMMED
NAZMUS SHAKIB
Date: 5 FEBRUARY 2021



SUPERVISOR'S DECLARATION

I hereby declare that I have checked this thesis and in my opinion this thesis is adequate in terms of scope and quality for the award of the degree in Bachelor of Engineering Technology (Electrical) with Honors.

(Supervisor's Signature)

Full Name : DR. MOHAMMED NAZMUS SHAKIB

Position : SENIOR LECTURER

Date : 5 FEBRUARY 2021



STUDENT'S DECLARATION

I hereby declare that the work in this thesis is based on my original work except for quotations and citations which have been duly acknowledged. I also declare that it has not been previously or concurrently submitted for any other degree at Universiti Malaysia Pahang or any other institutions.

(Student's Signature)

Full Name : ABDUL WAFIY BIN KASSIM

ID Number : TB17060

Date : 5 FEBRUARY 2021

**WIDEBAND MIMO ANTENNA DEVELOPMENT FOR
WIRELESS COMMUNICATION**

ABDUL WAFIY BIN KASSIM

Thesis submitted in partial fulfillment of the requirements for the
award of the degree of
Bachelor of Engineering Technology (Electrical) With Hons

Faculty of Electrical & Electronics Engineering Technology
UNIVERSITI MALAYSIA PAHANG

FEBRUARY 2021

ACKNOWLEDGEMENTS

I am sincerely grateful to ALLAH S.W.T for giving me strength, knowledge, patience, and guidance to complete my project work. Had it not been due to his will and power, the completion of this study would have been impossible.

This thesis would not have been possible without the assistance and guidance of certain individuals who contributed and extended their valuable effort in the preparation and the completion of this study. I am truly grateful to my supervisor, Dr Nazmus Shakib for his guidance, knowledge, ideas, critical comment, and encouragement which helped me in all the time of research, writing of this dissertation and help throughout my project work.

My grateful thanks also go to both of my parents Kassim bin Jaafar and Mizzah binti Ismail for their unconditional love and moral support from start until the end of my final year project. Finally, a special thanks to my partner, Muhammad Izzuddin bin Jauri, Muhammad Hafizuddin and all friends for their countless assistance and always there during our up and down during this project. It shows how strong our bonds are and I am grateful to have them.

ABSTRACT

This paper is focusing on filter designs capable of operating in 2.4GHz and 3.5GHz to 4.2GHz, the new radio frequency sub 6GHz. In this decade, it saturated with wireless technology resulting in increasing of wireless power density as there is an increasing number of electromagnetic (EM) sources such as cellular mobile base stations, digital TV towers and Wi-Fi transmitters. In recent years, the idea of using radio frequency (RF) power for low power electronic devices has been gaining momentum to replace batteries and save on maintenance costs. To begin with, an integrated device that include MIMO antenna, filter and energy harvesting circuit has been fabricated. In this dissertation, a microstrip dual-band bandpass is proposed and designed to operate at 2.4GHz and 3.5GHz to 4.2GHz without requiring any external impedance matching block. With two dual arms patch design and defected ground structure (DGS), the filter was designed using High Frequency Structure Simulator (HFSS). The simulation resulted in less return loss at the targeted frequency.

ABSTRAK

Laporan ini memfokuskan pada reka bentuk filter yang mampu beroperasi dalam 2.4GHz dan 3.5GHz hingga 4.2GHz, sub frekuensi radio baru 6GHz. Dalam dekad ini, ia dipenuhi dengan teknologi tanpa wayar yang mengakibatkan peningkatan kepadatan kuasa tanpa wayar kerana terdapat peningkatan jumlah sumber elektromagnetik (EM) seperti stesen pangkalan bergerak selular, menara TV digital dan pemancar Wi-Fi. Dalam beberapa tahun kebelakangan ini, idea menggunakan kuasa frekuensi radio (RF) untuk peranti elektronik berkuasa rendah telah mendapat momentum untuk mengganti bateri dan menjimatkan kos penyelenggaraan. Sebagai permulaan, peranti bersepadu yang merangkumi antenna MIMO, saringan dan penuaian tenaga telah dibuat. Dalam disertasi ini, jalur lebar dwi-jalur mikrostrip diusulkan dan dirancang untuk beroperasi pada 2.4GHz dan 3.5GHz hingga 4.2GHz tanpa memerlukan blok pencocokan impedans luaran. Dengan reka bentuk dua lengan tampalan dan struktur tanah yang cacat (DGS), penapis dirancang menggunakan Simulator Struktur Frekuensi Tinggi (HFSS). Simulasi tersebut mengakibatkan kehilangan pulangan lebih rendah pada frekuensi yang disasarkan.

TABLE OF CONTENT

DECLARATION	
TITLE PAGE	
ACKNOWLEDGEMENTS	ii
ABSTRACT	iii
ABSTRAK	iv
TABLE OF CONTENT	v
LIST OF TABLES	viii
LIST OF FIGURES	ix
LIST OF SYMBOLS	x
LIST OF ABBREVIATIONS	xi
LIST OF APPENDICES	xii
CHAPTER 1 INTRODUCTION	1
1.1 Project Background	1
1.2 Problem Statement	3
1.3 Objectives	4
1.4 Project Scope	4
CHAPTER 2 LITERATURE REVIEW	5
2.1 Introduction	5
2.2 Background	5
2.2.1 Bandpass Filter	5
2.2.2 Low-pass Filter	6
2.2.3 High-pass Filter	6

2.2.4	Band-stop Filter	7
2.3	Signal Processing Configuration	7
2.3.1	Butterworth Response	7
2.3.2	Chebyshev Response	8
2.4	Filter Design	8
2.4.1	Defected Stub Loader Resonator (DSLRL)	8
2.4.2	Multilayer Structure	9
2.4.3	Defected Ground Structure (DGS)	10
2.5	Substrate Material and Thickness	11
2.6	Conclusion	12
CHAPTER 3 METHODOLOGY		13
3.1	Introduction	13
3.2	Flowchart	14
3.3	System Developing process	15
3.4	Selection of Material	15
3.5	Calculation	16
3.6	Dual-Band Bandpass Filter	18
3.7	Defected Ground Structure (DGS)	20
3.8	Simulation	21
3.9	Conclusion	22

CHAPTER 4 RESULT DISCUSSION	223
4.1 Introduction	23
4.2 Simulation Result	24
4.3 Insertion losses	26
4.4 Conclusion	27
CHAPTER 5 CONCLUSION	28
5.1 Summary	28
5.2 Recommendation	28
REFERENCE	29
APPENDICES	31

LIST OF TABLES

Table 2.1	Phase lag for different filters with -20dB Attenuation at 200Hz.	8
Table 2.2	Variation of antenna with different substrate	12
Table 2.3	Variation of antenna with different substrate thickness.	12
Table 3.1	Dielectric substrate material	16
Table 4.1	Result for S_{11} and S_{22} .	27
Table 4.2	Result for S_{12} and S_{21} .	29

LIST OF FIGURES

Figure 1.1	Block diagram of RF energy harvesting system.	1
Figure 2.1	Ideal circuit	6
Figure 2.2	Structure of DSLR	9
Figure 2.3	Structure of multilayer BPF.	11
Figure 2.4	Variable characteristic impedance transmission line with DGS ground island and varactor diodes	11
Figure 3.1	Flowchart	15
Figure 3.2	Components of dual-band bandpass filter.	19
Figure 3.3	Dimension of microstrip patch.	20
Figure 3.4	Design of DGS.	21
Figure 3.5	Dimension of the DGS.	21
Figure 3.6	Top view of filter	22
Figure 3.7	Bottom view of filter.	23
Figure 4.1	S-parameter for S_{11}	25
Figure 4.2	S-parameter for S_{22} .	26
Figure 4.3	S-parameter for S_{12} .	28
Figure 4.4	S-parameter for S_{21} .	28

LIST OF SYMBOLS

Ω	Ohm
ϵ_{eff}	Effective dielectric constant
f	Operating frequency
ϵ_r	Dielectric constant
λ_m	Wavelength in millimetre
GHz	Giga hertz
η	Efficiency
f_c	Cutoff frequency
f	Operating frequency
MH	megaHenry
GHz	Gigabit Hertz
KHz	KiloHertz
dB	Gain
w	width

LIST OF ABBREVIATIONS

MIMO	Multiple Input Multiple Output
NR	New Radio
RF	Radio Frequency
TZ	Transmission Zero
5G	Fifth Generation
4G	Fourth Generation
3G	Third Generation
mm-Wave	Millimetre Wave
DC	Direct Current
WLAN	Wireless Area Network
EBG	Electromagnetic Bandgap
LPF	Lowpass Filter
BPF	Bandpass Filter
PCM	Parallel Coupled Microstrip
DSLRL	Defective Stub Loaded Resonator
HFSS	High Frequency Structure Simulator
DGS	Defected Ground Structure
mm	millimetre

LIST OF APPENDICES

Appendix A	Datasheet of substrate material	33
Appendix B	The fabricated filter	34
Appendix C	Prototype of the integrated device.	35
Appendix D	Photo of group member.	36
Appendix E	Presentation poster	37

CHAPTER 1

INTRODUCTION

1.1 Project Background

Over past two decades, wireless systems being developed and implemented to such an extent which frequency spectrum has become dense. These systems are Wi-Fi, cellular radio, radio broadcast and TV broadcast. Large amount of ambient energy (e.g. wind, solar and tide) is widely available and large-scale technologies developed efficiently to capture it. Hence, there are small amounts of “wasted” energy that prove to be useful if captured. Recovering even a fraction of this energy would have a significant environmental and economic impact. This is where energy harvesting (EH) comes from. The concept of energy harvesting is not new rather it came into picture 100 years back. The method of extracting energy from environment to generate electricity known as energy harvesting or energy scavenging. This technology offers two main advantages a) Energy is freely available b) It is "green" for the environment. The ambient energy present around us harvested using a rectifying antenna, popularly known as rectenna. RECTENNA is a rectifying antenna that used to convert electromagnetic energy into direct current electricity. The component of the energy harvesting system (antenna, matching network and rectifier) usually referred as a Rectenna, which is able to harvest high-frequency energy in free space and convert it to DC power. Harvesting RF energy and converting it into useful DC power requires careful design such as an efficient antenna designed to boost RF signal, a matching circuit to transfer maximum RF power from source to load and Rectifying circuit to convert input RF to DC.

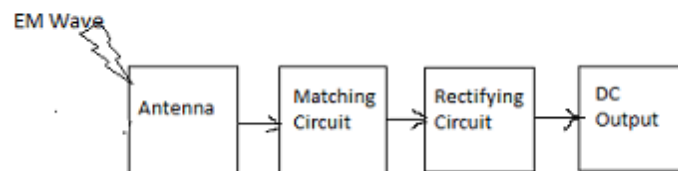


Figure 1.1: Block diagram of RF energy harvesting system.

MIMO systems improve communication performance by using multiple antennas at both the transmitter and the receiver. It is one of many forms of smart antenna technology. Hence, MIMO technology proposed for different communication systems such as WLAN systems, 3G and 4G cellular mobile systems. Since closely spaced antennas can cause strong mutual coupling, both mutual coupling and isolation can improve by increasing the distance between the antenna elements. However, the compact size of the wireless devices imposes limitations to this approach. Therefore, the remarkable challenge lies in the necessity of reducing the mutual coupling or enhancing the isolation between closely placed antennas' elements. A lot of methods already presented in the literature such as using etched slots on the ground, Defected Ground Structure (DGS), including the neutralization line, electromagnetic bandgap (EBG) structure, using metamaterial structures, and etching a slot in each of the feed lines.

Massive MIMO systems are extremely complex and implementing them will be harder than riding a bronco in the rodeo. However, the assets that massive MIMO have to offer worth thrown off the horse a few times. Firstly, spectral efficiency. This is becoming a very important topic as more and more of the electromagnetic spectrum being use for various communication protocols. Governments have set aside a wide band of frequencies for 5G, but those spectrums are not endless. Massive MIMO is able to leverage its antenna array to focus beams down to individual users. This allows it to achieve spectral efficiencies 10 times better than that of MIMO systems used for 4Gat. Secondly, energy efficiency. Texas will not be producing oil forever, so it is time to start thinking about energy efficiency for electronic systems as well. In massive MIMO antennas can be used in conjunction to increase the gain of transmitted signals. This means they radiate less power when transmitting data, making for a more energy efficient system. Lastly, user tracking. The same thing that makes massive MIMO energy efficient allows it to accurate track individual users. As the antenna beams are focused to produce high gain, their beam widths decrease. Thus, the tower has to track each user with a narrow signal beam. This tracking will give users a better and more reliable connection than the wide area signals that have been use up to now.

1.2 Problem Statement

Today's wireless technology obviously will not take us to the hyperactive accessibility with limitless communication at real-time speed from any mobile device with unlimited bandwidth. That is because of low network efficiency and lack of bandwidth. To improve the performance of a wireless communication network, the use of MIMO does not require a single antenna unit to solve this problem. Designing a MIMO antenna for communication, which requires antenna with high gain, precise directivity, and high efficiency, is also challenging work, which required MIMO antenna for dual band operation to overcome the limitation of single band.

Next Band Pass Filter is an important function commonly used in both transmitters and receivers. Thus, the quality of band pass filter is extremely important because it require filter to suppress signal noise. In designing the filter, need to find the specific physical dimension of the filter. Therefore, to get the filter that would be significantly smaller at the cost of less symmetric frequency response.

In addition, rectenna is a device that required energy harvesting by developing a rectifier that can convert RF energy from free space to DC power which able to sustain energy. Therefore, the key feature of the RF energy-harvesting device is the rectenna, which measures the ambient RF energy from the antenna and transforms the transmitted energy into DC electricity from the rectifier circuit. The rectifier needs harvest energy for 2.4GHz and 3.5GHz - 4.2GHz from filter and will convert into DC voltage.

1.3 Objectives

The main aim of this project is to develop wideband for wireless communication:

- To design wideband MIMO antenna for wireless communication.
- To develop MIMO antenna integrated filter for wireless communication in WLAN and New 5G NR frequency bands.
- To evaluate integrated device for energy harvesting system.

1.4 Project Scope

MIMO (multiple input, multiple output) is an antenna technology for wireless communications in which multiple antennas are used at both the source (transmitter) and the destination (receiver) to gain knowledge of communication channel. Besides, single antenna cost more and big size which is not compact. Compare to dual band, it can reduce the system size and cut the system cost. Therefore, MIMO require filter to suppress the noise signal. This is because antenna and filter are two indispensable devices in RF front-end.

Other than that, integrate energy harvesting can give benefit to the rural area such as streetlamp and supply the energy. The 5G New Radio (5G NR) is a brand-new air interface can be considered as the technology used for the communication link between mobile devices and the base station within a cellular network. Hence, energy harvesting can be save more energy. This is because RF energy, which is free cost that collected on free space. This method we can apply at the rural areas that does not have many signal towers. The rectifier is to harvest RF energy for 2.4GHz and 3.5GHz – 4.2GHz frequency from the filter that will convert to DC voltage.

CHAPTER 2

LITERATURE REVIEW

2.1 Introduction

An RF front end is required in most communications systems, where low noise amplifiers and RF filters perform analogue signal processing. RF filters for microstrips are frequently used in running receivers and transmitters in the frequency range of 800 MHz to 30 GHz. The parallel coupling line and the interdigital filter are the most common form used. Another variant of the parallel coupled is a hairpin filter where the resonators are bent into the form of a hairpin to accomplish a more suitable aspect ratio. The architecture of these filters (C. J. Kikkert, 2008) are well known and typically involve the use of relationships with empirics. Filters with microwave RF are built using low pass filter equations (C. J. Kikkert, 2008) convenient transformations or with the use of coupled resonators design procedures.

2.2 Types of filter

2.2.1 Bandpass Filter

In modern wireless communication systems, high performance bandpass filters (w lans) with low insertion loss within the passband and high out-of-band suppression are widely desired. By adding several transmission zeros (TZs), the out-of-band characteristics are usually improved. In (K. D. Xu, F. Zhang, Y. Liu, Q. H. Liu, 2018), two tunable TZs, both of which are located at the lower stopband or upper stopband, are used to improve stopband suppression. The number of TZs is obviously not enough to fulfill the rejection of both the lower and upper stopbands simultaneously. The definition of the TZ resonator pair is proposed in (K. D. Xu, F. Zhang, Y. Liu, Q. H. Liu, 2018), where the positions of four TZs are precisely at the resonant frequency points of the two pairs of resonators. The lower stopband does not suppress very well due to its structure constraint. In addition, transversal signal interference techniques are used to implement two or more transmission paths with multiple TZs for the BPF design, but at the cost of the increase in overall scale.

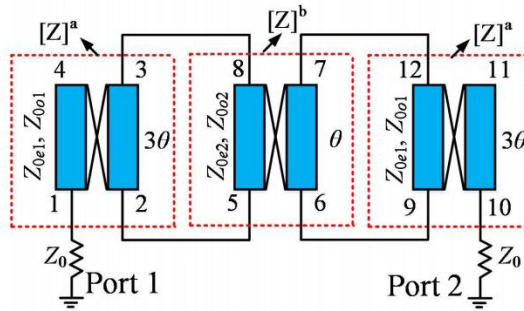


Figure 2.1: Ideal circuit

2.2.2 Low-pass Filter

Low Pass filters are filters that allow the passage of low frequency signals and attenuate high frequency signals. Lately, microstrip low pass filter (LPF) are widely known and its creation to make it simple, compact, and inexpensive. Planar LPFs are especially common because they can be calculated. It uses printed circuit technology and is suitable for industrial use. Various approaches to achieving a large stop band region on low pass filters have been published in the literature.

Filters are for low frequency exclusion that can interfere with the system, so that only the selected frequency can break out of the system. Low pass filter open stubs are intended to distribute and produce frequency on that device. It is possible to have different stub sizes on one device, and each stub represents one resonant (Gunawan, Wahyu, Oktafiani, 2017).

2.2.3 High-pass Filter

The filter for the high pass is the exact opposite of the filter for the low pass. Up to a defined cut-off frequency (f_c) point, this filter has no output voltage from the DC. 70.707% of the lower cut-off frequency point (f_c) or -3dB ($\text{dB} = -20 \log(V_{\text{out}}/V_{\text{in}})$) of the voltage gain was allowed to pass. The "below" frequency range of this cut-off frequency point f_c is generally

referred to as the stop band, whereas the "above" frequency range of this cut-off frequency point is generally referred to as the pass band. You will find the cut-off frequency or point of -3dB using the formula $f_c=1/(2\pi RC)$. The output signal phase angle at (f_c) is $+45^\circ$. The high pass filter is usually less distorting than its low pass filter counterpart (Hui Chen, Di Jiang, Ke-Song Chen, Hong-Fei Zhao, 2016).

In audio amplifiers, a very common use of a passive high pass filter since a coupling capacitor between two stages of audio amplifiers and that of the speaker systems in the audio amplifier is used to direct the high-frequency signals to the smaller "tweeter" style speakers. In order to minimize any low noise or "rumble" style distortion, it blocks the lower bass signals. The high-pass filter is often referred to as a low-cut or bass-cut filter when used in audio applications (Rinchen Khando, 2012).

2.2.4 Band-stop Filter

A switchable band-stop filter, a sensing bandpass filter, a sensing analogue circuit, and a switch driving circuit co-design allow all-pass-to-band-stop switchable filters to be triggered automatically when power is present within the filter's bandwidth above a designable threshold. To test the technique at 2.15 GHz, a third order suspended-stripline power-activated switchable all-pass to band-stop filter with a second-order resonant power sensor was developed and measured. There is less than 1.7 dB insertion loss in the calculated all-pass state, while the automatically switched band-stop state offers more than 18 dB attenuation (E. J. Naglich, S. Shin, 2018).

2.3 Signal Processing Configuration

2.3.1 Butterworth Response

Butterworth filters are called maximally flat filters because, without causing peaking in the Bode plot, they have the sharpest roll-off possible for a given order. The second-order Butterworth filter is a two-pole filter with a 0.707 damping ratio. In control systems, Butterworth filters are used because they do not have peaks. There is a conservative necessity to exclude all

peaks from a filter. It can be helpful to enable some peaking because it allows equal attenuation in the lower frequencies with less phase lag; this has been shown in Table 2.1. The Butterworth filter is, however, a natural choice for organizing the many higher-order filter poles used in control systems (George Ellis, 2012).

Table 2.1: Phase lag for different filters with -20dB Attenuation at 200Hz.

Filter Order	Damping Ratio	Filter Bandwidth	Attenuation at 200 Hz	Phase Lag at 20 Hz
1	N/A	21 Hz	20 dB	43°
2	1.0	66 Hz	20 dB	33°
2	0.7	63 Hz	20 dB	26°
2	0.4	60 Hz	20 dB	16°

2.3.2 Chebyshev Response

To separate one frequency band from another, Chebyshev filters are used. Although they are unable to match the windowed-sinc filter efficiency, they are more than adequate for many applications. The primary attribute of Chebyshev filters is their speed, usually faster than the windowed-sinc by more than an order of magnitude. This is because they are carried out not by convolution, but by recursion. The Chebyshev response is a mathematical technique for achieving a faster roll off by allowing ripple in the frequency response. Chebyshev filters are called analogue and digital filters that use this technique (Steven W. Smith, 2003).

2.4 Filter Design

2.4.1 Defected Stub Loaded Resonator (DSLRL)

The configuration of the proposed defective stub-loaded resonator (DSLRL) unit is shown in Figure 1 as the white portion on the bottom layer consisting of a defective open-loop resonator and a center-loaded defective stub. The DSLRL is very similar to the dual-mode stub-loaded resonator (SLR), except for those where the proposed resonator is performed by etching an SLR on the L₁, L₂, and H and W₁ and W₂ represent the defective physical lengths and widths of each

of the DSLR sections, respectively, and g denotes the open gap width. For design convenience, $W_2 = 2W_1$ is presumed. It should be noted here that the DSLR can be interpreted as many slot lines and as the microstrip ones have opposite impedance characteristics. This implies that a narrow W_1 results in a lower impedance, while a wide W_2 results in a higher impedance (Dechang Huang, Zhaodi Huang, 2014).

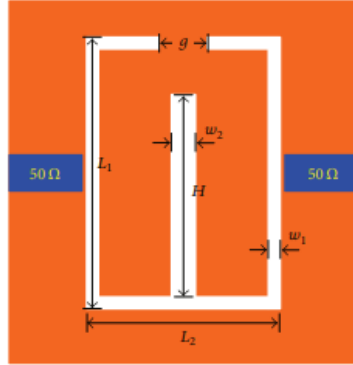


Figure 2.2: Structure of DSLR

2.4.2 Multilayer Structure

Two wideband bandpass filters and compatible circuits make up this bandpass filter. A class of controllable response wideband dual band BPFs was proposed in (Majidifar, Sohrab, Makki, Seyed Vahab AL-Din, 2015). Two multi-mode resonators (MMRs) with short-circuited stubs were connected in parallel in this approach to form the fundamental structure of the proposed dual-band BPF.

One of the dual-band BPFs (method 2) direct design techniques created by adding a bandstop filtering response between a large passband to break it into two passbands. In a cascade relation, a dual-band filter comprises a bandstop filter and a wideband bandpass filter. Two equal bandpass resonators (R_1 and R_2), which are coupled together, make up this structure. With the relative dielectric constant of ϵ_r and thickness of $2H$, the first resonator is mounted on a substrate

and the top layer of this resonator is free space. Two substrates with a relative dielectric constant of ϵ_r surround the second resonator (Majidifar, Sohrab, Makki, Seyed Vahab AL-Din, 2015).

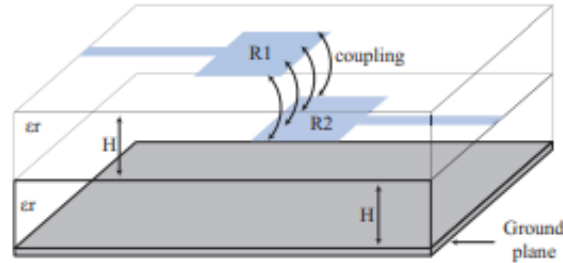


Figure 2.3: Structure of multilayer BPF.

2.4.3 Defected Ground Structure

One of the main components in multi-service wireless communication systems is BPFs that have tunable multi-band capabilities. In the design of BPF, stub loaded resonators are widely used. In the design of multi-band BPFs, multi-mode resonators, such as stepped impedance resonators (SIRs) and stub loaded open loop resonators, have recently been used. The specification of tunable dual-band BPFs is also of great importance.

A centrally loaded varicose diode in a resonator half-wavelength and the SIR loaded capacitor were presented in the design of the tunable BPF. However, in order to tune the center frequency of the BPFs, these techniques are often based on the use of variable reactance components. Transmission lines with changed soil structure, such as a photonic band gap and a DGS, were actively studied and successfully implemented in the design of different microwave circuits (Chaudhary, Girdhari, Choi, Heungjae, Jeong, Yongchae, Lim, Jongsik, Kim, Dongsu, Kim, Jun-Chul, 2011).

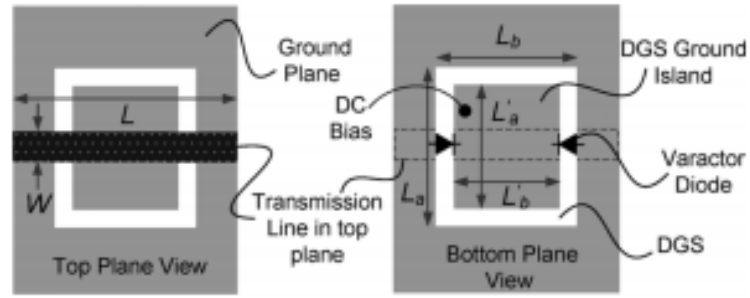


Figure 2.4: Variable characteristic impedance transmission line with DGS ground island and varactor diodes

2.5 Substrate Material and Thickness

During designing the filter, the material for the substrate must be decided. Different material has different dielectric constant, ϵ_r . It is advised to have material that has lower dielectric constant to have better performance. The key drawback of a microstrip antenna is the inherently limited bandwidth of impedance. While we used a rectangular patch, the radiating patch may be of any geometric configuration, such as square, rectangle, circular, elliptical, triangular, E-shaped, H-shaped, L-shaped, U-shaped, etc.

The material containing the dielectric constant can be used as a substrate in the range of $2.2 \leq \epsilon_r \leq 12$. As we change the substrate material and the substrate thickness of a microstrip antenna, the performance changes. Hence, in order to implement suitable design of the antenna, it is essential to understand the effect of changing the material of the dielectric substrate and thickness of substrate (Liton Chandra Paul, Sohag Sarker, Md Sarwar Hosain, 2015).

Table 2.2: Variation of antenna with different substrate.

Substrate Material Name	Dielectric constant ϵ_r	Length of Patch L_p (mm)	Width of Patch W_p (mm)	Inset depthd(mm)	Resonance frequency f_r (GHz)	Directivity D (dB)	GainG(dB)	Return lossR(dB)	Bandwidth BW(MHz)
RT Duroid 5880	2.2	41.408	49.410	12.398	2.406	7.00870	7.00410	-19.402	30.5
GML 1000	3.2	34.483	43.129	11.312	2.411	6.38395	6.37818	-41.363	26
RO4003	3.4	33.472	42.137	11.126	2.408	6.30076	6.29490	-27.994	25
FR-4	4.4	29.479	38.036	10.321	2.408	5.98928	5.68109	-20.516	22

Table 2.3: Variation of antenna with different substrate thickness.

h (mm)	L_p (mm)	d (mm)	f_r (GHz)	D (dB)	G (dB)	R (dB)	BW (MHz)
0.5	41.932	12.555	2.421	6.88037	2.62412	-0.836	
1	41.685	12.481	2.406	6.90260	2.69583	-1.316	
1.3	41.522	12.432	2.398	6.91738	2.76126	-1.651	
1.5	41.408	12.398	2.410	7.00735	7.00274	-27.221	31.5
2	41.106	12.308	2.403	7.02175	7.01743	-21.196	44
2.5	40.784	12.212	2.394	7.03605	7.03202	-19.637	56
3	40.448	12.110	2.384	7.04630	7.02344	-20.059	68
3.5	40.099	12.006	2.372	7.06027	7.00487	-22.496	81
4	39.741	11.899	2.362	7.07394	6.98569	-28.280	91
4.5	39.374	11.789	2.354	7.08734	6.96575	-39.232	99

2.6 CONCLUSION

In this chapter, the author has explained about the concept and technique that have used in this project for making dual band bandpass filter.

CHAPTER 3

METHODOLOGY

3.1 Introduction

In order to accomplish the purpose of this project, this chapter focuses on the processes and procedures that need to be performed. In every aspect, the methods chosen were considered to ensure a satisfactory outcome of the dual bandpass filter. This project starts by designing the workflow of the project and it is possible to complete a literature analysis of the project on time, the scheduling must be carried out and must also act as a guideline for the project's work schedule.

3.2 Flowchart

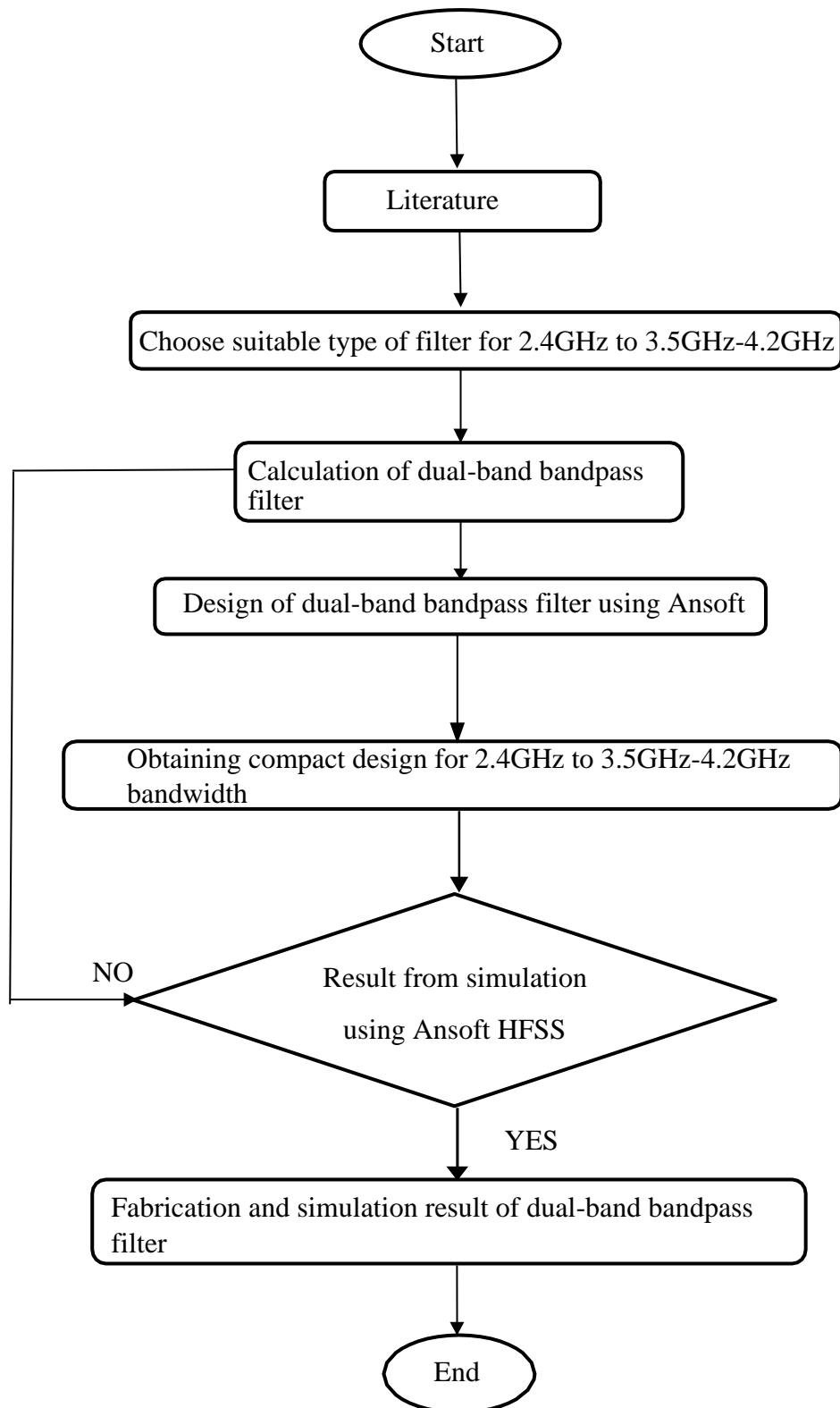


Figure 3.1: Flowchart of the project.

3.3 System developing process

The dual-band bandpass filter is crucial to suppress the noise and remove unwanted frequency coming from the MIMO antenna. The filter has been designed using High Frequency Structure Simulator (HFSS) to simulate and get the result. It was designed with two dual arms microstrip line to achieve the compactness of the filter. A suitable substrate material was chosen to get the required frequency of 2.4GHz and 3.5GHz to 4.2GHz. Other than that, the defected ground structure was input for the ground of the filter to achieve the frequency.

3.4 Selection of dielectric material

The choice of the dielectric substrate needed to build the filter required low frequency suitability, efficiency, loss gain, and filter compactness to be achieved. Table 3.1 displays the selected substrate material with its tangent loss, resonance frequency and relative substrate permittivity. This material is very critical for achieving efficiency at the target frequency of 2.4GHz and 3.5GHz to 4.2GHz.

Table 3.1: Dielectric substrate material

Substrate	ϵ_r	Dissipation Factor, $\tan \delta$
Rogers RT/Duroid® 5880	2.2	0.0004 0.0009

3.5 Calculation

To design dual-band bandpass filter using microstrip, specific criteria of the microstrip such as width of the conductor, wavelength, the velocity phase needed to determine before fabrication process begin. The effective dielectric constant is a function of the relative permittivity of the substance, the substrate thickness and the conductor width. It can be approximately determined using these formulas.

$$\epsilon_{eff} = \frac{\epsilon_r + 1}{2} + \frac{\epsilon_r - 1}{2} * \left(\frac{1}{\sqrt{1 + 12D/W}} \right) \quad (1)$$

Where:

ϵ_{eff} = effective dielectric constant ϵ_r

= relative permittivity of substrate

The wavelength, λ_m (mm) in the microstrip is related to the phase velocity and can be determined using:

$$\lambda_m = \frac{300}{F \sqrt{\epsilon_{eff}}} \quad (2)$$

Where:

λm = wavelength in millimetres

f = intended frequency of operation in

GHz ϵ_{eff} = effective dielectric constant

The ratio of conductor width to dielectric thickness can be determined for a given characteristic impedance and relative permittivity using the following equation given:

$$\frac{W}{D} = \begin{cases} \frac{8e^A}{e^{2A} - 2} & \text{for } \frac{W}{D} < 2 \\ \frac{2}{\pi} \left[B - 1 - \ln(2B - 1) + \frac{\epsilon_r - 1}{2\epsilon_r} \left\{ \ln(B - 1) + 0.39 - \frac{0.61}{\epsilon_r} \right\} \right] & \text{for } \frac{W}{D} > 2 \end{cases} \quad (3)$$

Where:

$$A = \frac{Z_0}{60} \sqrt{\frac{\epsilon_r + 1}{2} + \frac{\epsilon_r - 1}{\epsilon_r + 1} \left(0.23 + \frac{0.11}{\epsilon_r} \right)} \quad (4)$$

$$B = \frac{377\pi}{2Z_0\sqrt{\epsilon_r}} \quad (5)$$

Using the equation given above, the length of microstrip for the quarter wave transformer and the input and output feedline length as well as the width are calculated according to the target frequency of 2.4GHz and 3.5GHz to 4.2GHz.

3.6 DUAL-BAND BANDPASS FILTER

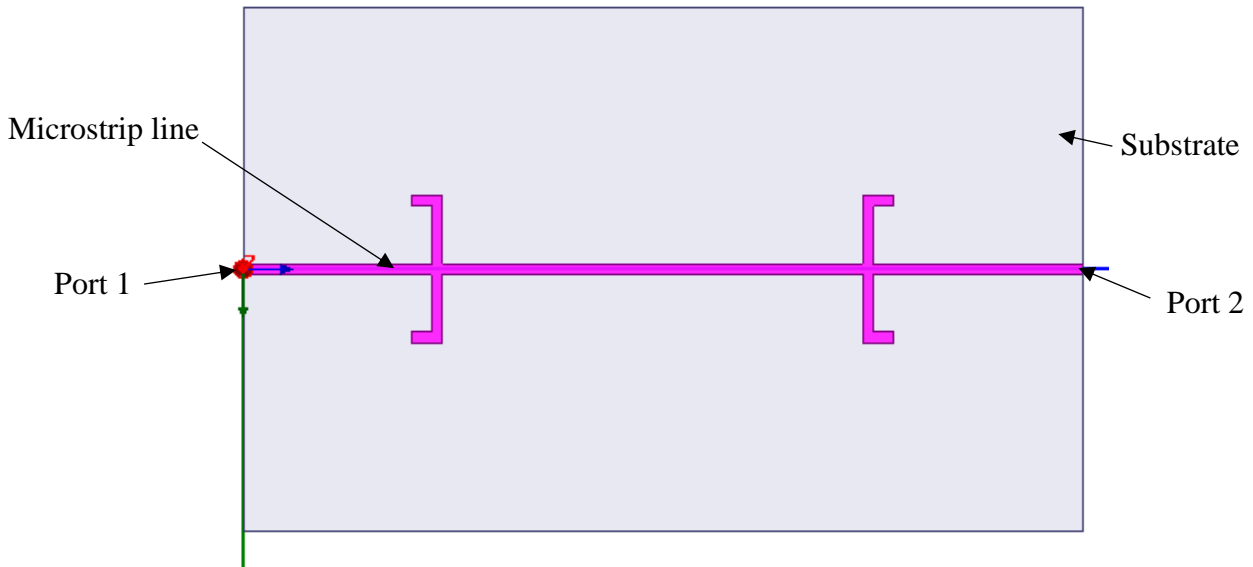


Figure 3.2: Components of dual-band bandpass filter.

The Roger RT/Duroid 5880 dielectric filter with a thickness of 1.6 mm is used for this filter. The concept was built with 2 techniques; the stepped impedance resonator ladder was combined with the technique of coupling. The microstrip consists of a thin 0.5 mm copper film etched on the surface of a filter dielectric substrate. For impedance matching purposes, different width of the microstrip imply the difference impedance being applied on the surface. The filter has 2 ports, which are Port 1 for input and Port 2 for output. The radio frequency (RF) of this filter was collected from the antenna via port 1 and filtered. After the radio frequency (RF) is filtered, it will submit to energy harvesting through Port 2.

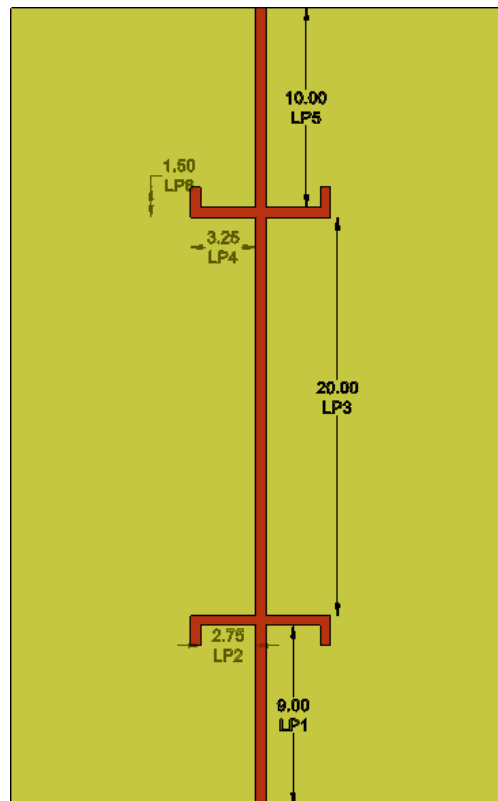


Figure 3.3: Dimension of microstrip patch.

The final dimension of the dual-band bandpass filter dielectric substrate is 40mm x 25mm. This dual-band bandpass filter has double two arms along the straight microstrip line. The arms are both identical but have different distance from the middle. The first arms are nearer to the front end of the substrate compare to the second arms with the rear end. At the end of each arms, it has a line notch. The microstrip line was made into a straight-line pattern only because it is possible to achieve faster simulation results compared to if the bend was inserted into the dual-band bandpass filter.

3.7 Defected Ground Structure

Using the Defected Ground Structure (DGS) method is one of the modern concepts linked to the dispersed microwave channel circuit. It can typically be achieved by altering the ground plane of a microstrip circuit intended to enhance execution, as shown in Figure 3.4. The DGS is used after the desired passband on the ground plane to evacuate the spurious display. In ground plane, such DGS units are used to keep up sure to remove harmonic s and get broad stopband. The rectangular will be positive to use in this paper since it is easy to use and formed. For this filter, the DGS were design with gap at the top and bottom end of the substrate. Then, there is extra rectangular gap at the top end of substrate. Apart from that, near the center of ground plane, there are two rectangular gaps with different parameter.

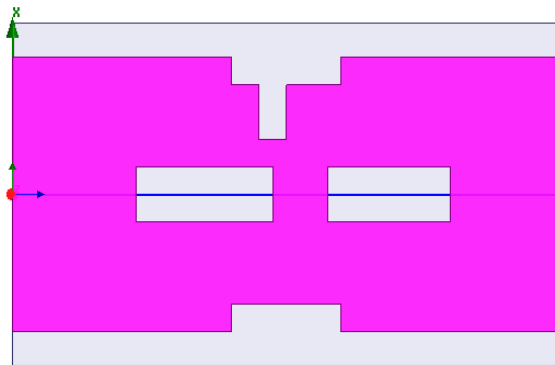


Figure 3.4: Design of DGS.

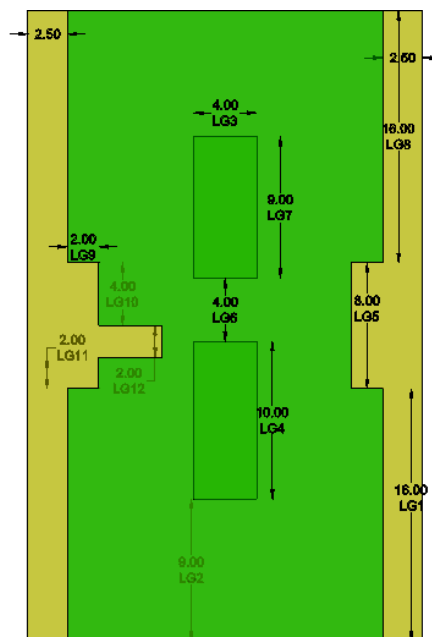


Figure 3.5: Dimension of the DGS.

3.8 Simulation

The dual-band bandpass filter was developed by using the high frequency structure simulator, (HFSS) Software 15.0. To get the required result, the S-parameter were evaluated, and the design was refined. The initial concept is shown in Figures 3.4 and 3.5 and the dual-band bandpass filter model is illustrated in the HFSS. This HFSS simulation was achieved through video tutorials obtained from the internet and through notes and paper regarding on how to design filters. The dual-band bandpass filter achieved the 2.4GHz and 3.5GHz to 4.2GHz frequency after many tweaking processes by adjusting all criteria such as microstrip size, ground plane and the feed line.

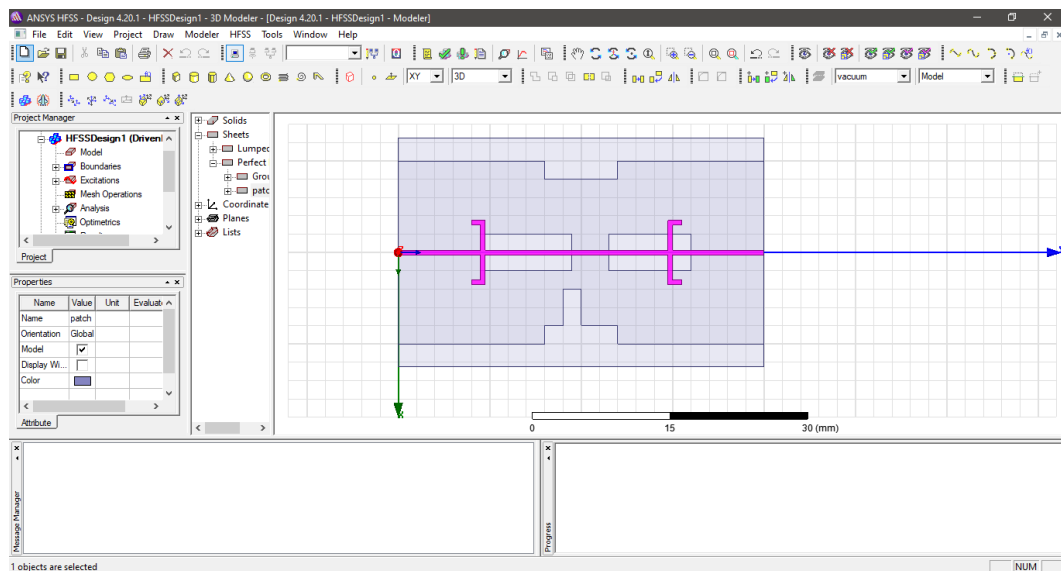


Figure 3.6: Top view of filter.

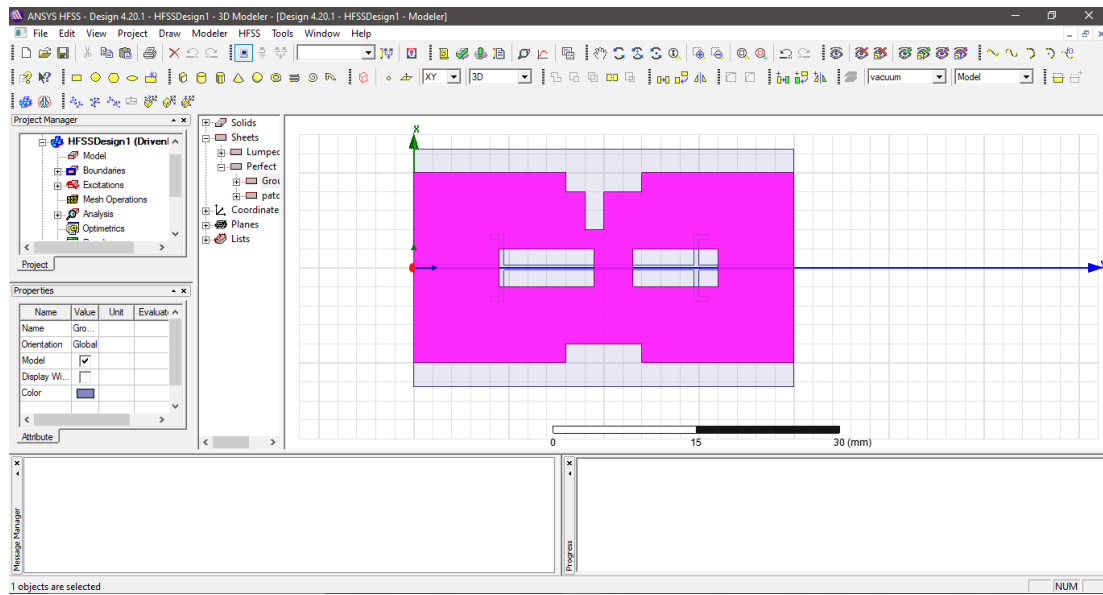


Figure 3.7: Bottom view of filter.

3.9 Conclusion

The dual-band bandpass filter design needs certain parameters for method of guideline for it to be ideal. It is desired that the measurement needed to secure the minimum possible dimension for the dual-band bandpass filter will be achieved. In the next chapter, the dual-band bandpass filter layout requires some improvement to display the results on this filter hitting the target frequency of 2.4GHz and 3.5GHz to 4.2GHz.

CHAPTER 4

RESULT AND DISCUSSION

4.1 Introduction

The simulation resulted from the Ansoft High Frequency Structure Simulator (HFSS) software of the dual-band bandpass filter will determine the input port and output port base around the S-parameter. Apart from that, the result project the return loss for require frequency of 2.4GHz and 3.5GHz to 4.2GHz to determine the efficiency of the dual-band bandpass filter.

4.2 Simulation Result

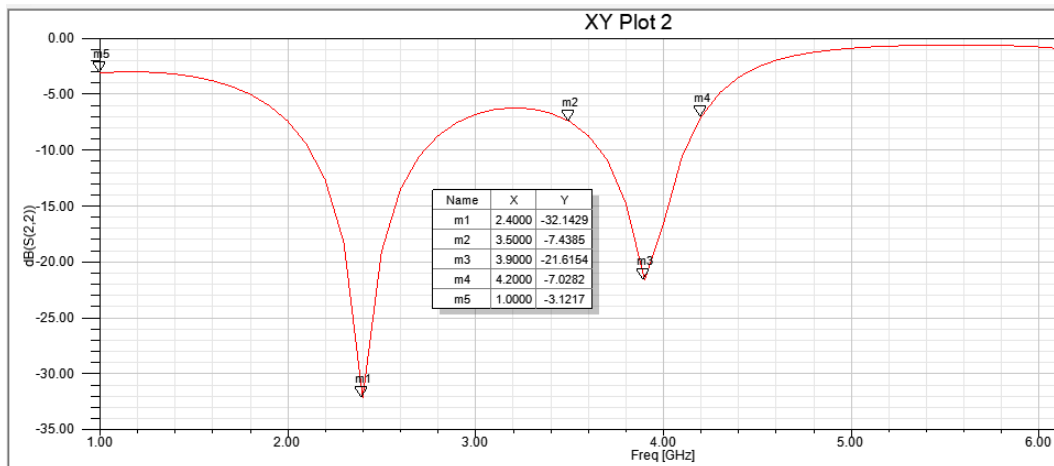


Figure 4.1: S-parameter for S_{11}

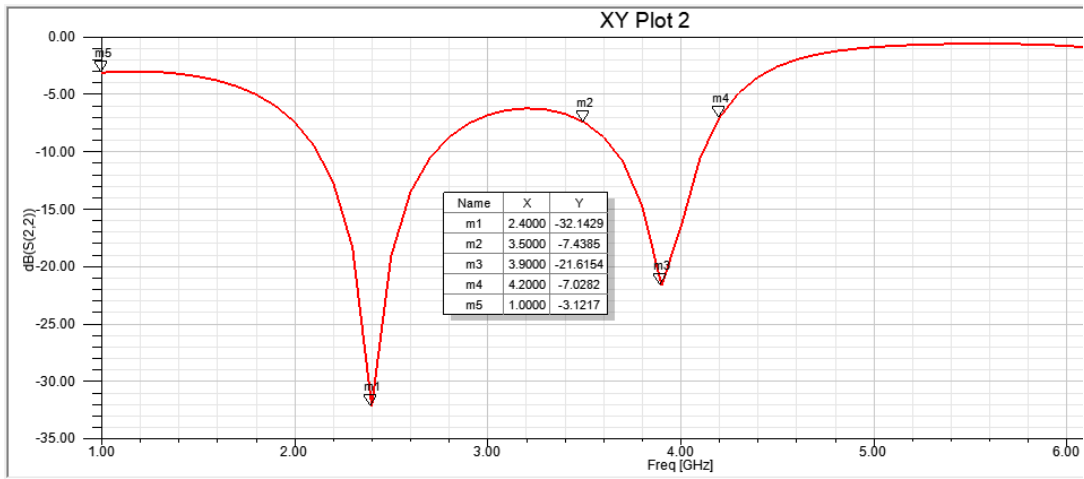


Figure 4.2: S-parameter for S22.

Table 4.1: Result for S₁₁ and S₂₂.

S-parameter	Frequency (GHz)	Coefficient Value (dB)
S ₁₁	2.4	-32.1249
	3.5	-7.4385
	3.9	-21.6154
	4.2	-7.0282
S ₂₂	2.4	-32.1249
	3.5	-7.4385
	3.9	-21.6154
	4.2	-7.0282

The value of each S-parameter having a value of or less than -10 dB for S₁₁ and S₂₂, which in turn has less reflection coefficient from each filter port. The reflectance coefficient shows the matching impedance of the dual-band bandpass filter at each port, the lower the value of the dual-band bandpass filter impedance matching. The broad impedance matching was achieved in this case, leading to less system losses.

4.3 Insertion Loss

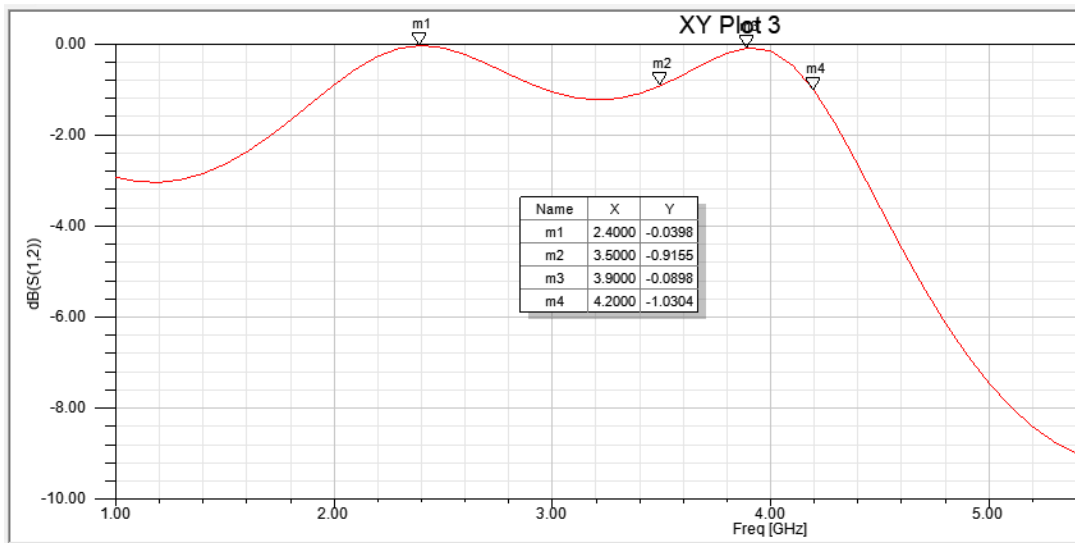


Figure 4.3: S-parameter for S₁₂.

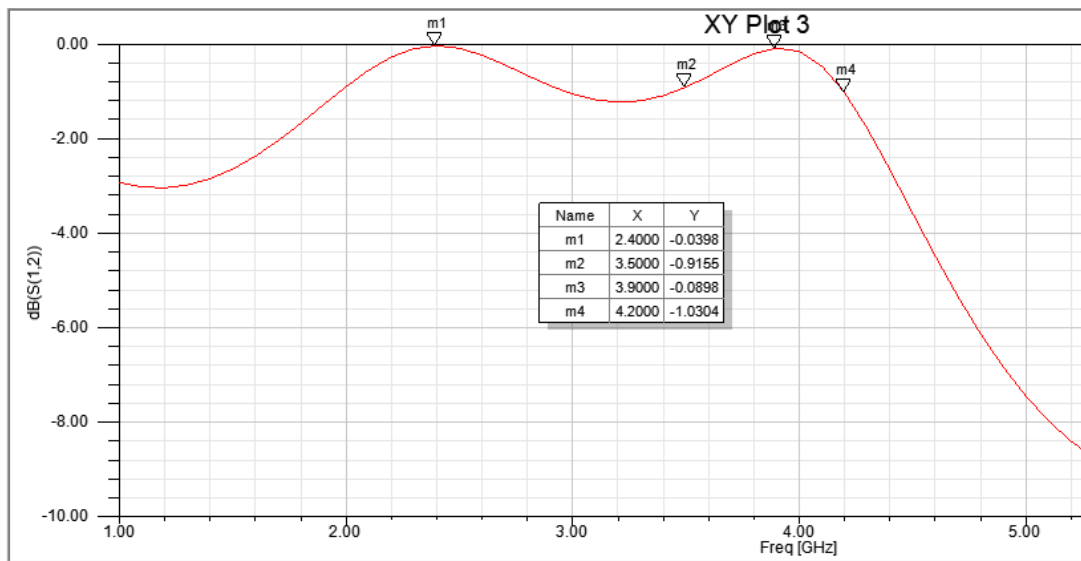


Figure 4.4: S-parameter for S₂₁.

Table 4.2: Result for S_{12} and S_{21} .

S-parameter	Frequency (GHz)	Coefficient Value (dB)
S_{12}	2.4	-0.0398
	3.5	-0.9155
	3.9	-0.0898
	4.2	-1.0304
S_{21}	2.4	-0.0398
	3.5	-0.9155
	3.9	-0.0898
	4.2	-1.0304

For S_{12} and S_{21} , the value of each S-parameter has a round value of -1dB for the targeted frequency, which resulted less insertion loss between the input port and the output port. The closer to the value to 0dB, more efficient the dual-band bandpass filter work with insertion loss.

4.4 Conclusion

In summary, the use of the scattering S- parameter in the filter helps to define the main elements of the dual-band bandpass filter. The design of the filter is based on the measured microstrip patch, the substrate material chosen and the crucial dimension before the dual-band bandpass filter is designed. Finally, aspects such as the reflection coefficient, isolation and the value of insertion losses have different effects on the general dual-band bandpass filter efficiency.

CHAPTER 5

CONCLUSION AND RECOMMENDATION

5.1 Summary

The objective of this thesis is to design and developed a compact size filter to suppress the noise of the targeted frequency which are 2.4GHz and 3.5GHz to 4.2GHz. The filter has a dimension of 40mm x 25mm x 1.6mm for the length, width, and thickness respectively. The material used for the filter is RT/Duroid 5880 has a dielectric constant of 2.2. Based on the simulation, the S-parameter S11 and S22 show that it has less than -10dB at the targeted frequency which in turn has less reflect coefficient. As for the S-parameter S12 and S21, the value of each S-parameter has a round value of -1dB for the targeted frequency, which resulted less insertion loss between the input port and the output port. The closer to the value to 0dB, more efficient the dual-band bandpass filter work with insertion loss. At the end of the project, the MIMO antenna and energy harvesting circuit were integrated with filter indicated the completion of the project.

5.2 Recommendation

To improve the performance of the filter, these recommendations were proposed:

- i. The filter can be improved by changing the material used for the substrate, adjusting the dimension of the substrate, or modifying the design of the patch to get better return loss.
- ii. Modify the MIMO antenna into 2 signal port instead of 4 signal port.
- iii. Use a better-quality power divider and other electrical components for the energy harvesting circuit.

REFERENCES

C. J. Kikkert, "A Design Technique for Microstrip Filters," 2008 2nd International Conference on Signal Processing and Communication Systems, Gold Coast, QLD, 2008, pp. 1-5, doi: 10.1109/ICSPCS.2008.4813713.

K. D. Xu, F. Zhang, Y. Liu and Q. H. Liu, "Bandpass Filter Using Three Pairs of Coupled Lines With Multiple Transmission Zeros," in IEEE Microwave and Wireless Components Letters, vol. 28, no. 7, pp. 576-578, July 2018, doi: 10.1109/LMWC.2018.2835643.

Gunawan, Wahyu & Oktafiani, Fitri & Sugeng, Bambang & Lukman,. (2017). Low Pass Filter Design With Artificial Ground Structure. Jurnal Sains Terapan. 3. 75-77. 10.32487/jst.v3i2.266.

Hui Chen, Di Jiang, Ke-Song Chen, and Hong-Fei Zhao, (2016) "A Compact High-Pass Filter Using Hybrid Microstrip/Nonuniform CPW with Dual-Mode Resonant Response"

Rinchen Khando, "High Pass Filter", 2012 Electronics and Communication Engineering Department College of Science and Technology Royal University of Bhutan

E. J. Naglich and S. Shin, "Power-Dependent Bandstop Filters for Wide-Bandwidth, High-Speed Interference Suppression," 2018 IEEE International Symposium on Antennas and Propagation & USNC/URSI National Radio Science Meeting, Boston, MA, 2018, pp. 1239-1240, doi: 10.1109/APUSNCURSINRSM.2018.8609156.

George Ellis, Chapter 9 - Filters in Control Systems, Editor(s): George Ellis, Control System Design Guide (Fourth Edition), Butterworth-Heinemann, 2012, Pages 165-183, ISBN 9780123859204.

Steven W. Smith, CHAPTER 20 - Chebyshev Filters, Editor(s): Steven W. Smith, Digital Signal Processing, Newnes, 2003, Pages 333-342, ISBN 9780750674447.

Dechang Huang and Zhaodi Huang, "Design of Dual-Band Bandpass Filter Using Dual-Mode Defected Stub Loaded Resonator", 2014

Majidifar, Sohrab & Makki, Seyed Vahab AL-Din. (2015). Dual Band Bandpass Filter Using Multilayer Structure. *Applied Computational Electromagnetics Society Journal*. 30. 1096-1101.

Chaudhary, Girdhari & Choi, Heungjae & Jeong, Yongchae & Lim, Jongsik & Kim, Dongsu & Kim, Jun-Chul. (2011). Design of Dual-Band Bandpass Filter Using DGS With Controllable Second Passband. *IEEE Microwave and Wireless Components Letters - IEEE MICROW WIREL COMPON LETT*. 21. 589-591. 10.1109/LMWC.2011.2167140.

Paul, Liton & Hosain, Md & Sarker, Sohag & Prio, Makhluq Hossain & Morshed, Monir & Sarkar, Ajay. (2015). The Effect of Changing Substrate Material and Thickness on the Performance of Inset Feed Microstrip Patch Antenna. *American Journal of Networks and Communications*. 4. 54-58. 10.11648/j.ajnc.20150403.16.

APPENDICES

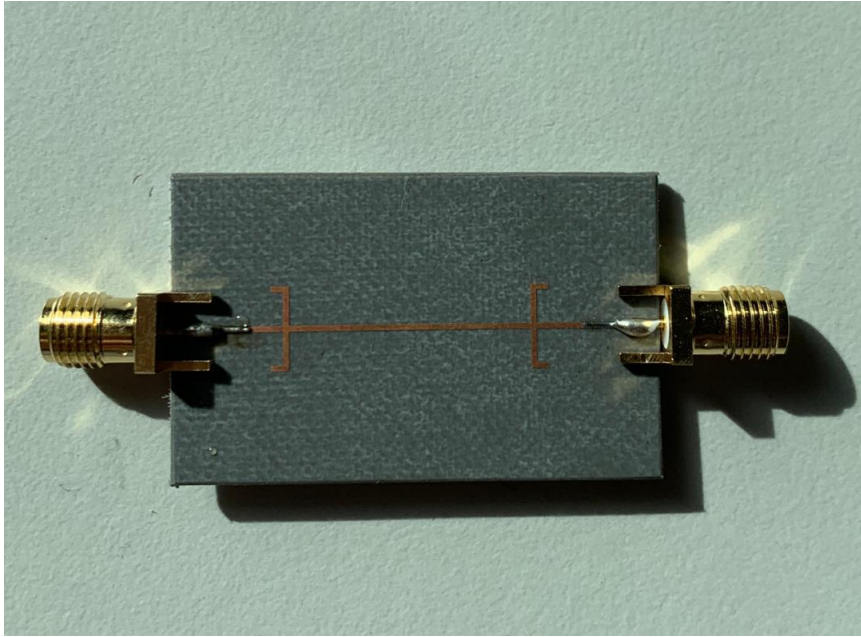
APPENDIX A

Datasheet of substrate material .

PROPERTY	TYPICAL VALUES				DIRECTION	UNITS ⁽¹⁾	CONDITION	TEST METHOD
	RT/duroid 5870		RT/duroid 5880					
⁽¹⁾ Dielectric Constant, ϵ_p Process	2.33		2.20		Z	N/A	C24/23/50	1 MHz IPC-TM-650 2.5.5.3 10 GHz IPC-TM-2.5.5.5
	2.33 ± 0.02 spec.		2.20 ± 0.02 spec.		Z	N/A	C24/23/50	
⁽¹⁾ Dielectric Constant, ϵ_p Design	2.33		2.20		Z	N/A	8 GHz - 40 GHz	Differential Phase Length Method
Dissipation Factor, tan δ	0.0005 0.0012		0.0004 0.0009		Z Z	N/A	C24/23/50 C24/23/50	1 MHz IPC-TM-650, 2.5.5.3 10 GHz IPC-TM-2.5.5.5
Thermal Coefficient of ϵ_p	-115		-125		Z	ppm/°C	-50 - 150°C	IPC-TM-650, 2.5.5.5
Volume Resistivity	2 X 10 ⁷		2 X 10 ⁷		Z	Mohm cm	C96/35/90	ASTM D257
Surface Resistivity	2 X 10 ⁷		3 X 10 ⁷		Z	Mohm	C/96/35/90	ASTM D257
Specific Heat	0.96 (0.23)		0.96 (0.23)		N/A	J/g/K (cal/g/°C)	N/A	Calculated
Tensile Modulus	Test at 23 °C	Test at 100 °C	Test at 23 °C	Test at 100 °C	N/A	MPa (kpsi)	A	ASTM D638
	1300 (189)	490 (71)	1070 (156)	450 (65)	X			
	1280 (185)	430 (63)	860 (125)	380 (55)	Y			
ultimate stress	50 (7.3)	34 (4.8)	29 (4.2)	20 (2.9)	X	MPa (kpsi)	A	ASTM D695
	42 (6.1)	34 (4.8)	27 (3.9)	18 (2.6)	Y			
ultimate strain	9.8	8.7	6.0	7.2	X	%	A	ASTM D695
	9.8	8.6	4.9	5.8	Y			
Compressive Modulus	1210 (176)	680 (99)	710 (103)	500 (73)	X	MPa (kpsi)	A	ASTM D695
	1360 (198)	860 (125)	710 (103)	500 (73)	Y			
	803 (120)	520 (76)	940 (136)	670 (97)	Z			
ultimate stress	30 (4.4)	23 (3.4)	27 (3.9)	22 (3.2)	X	MPa (kpsi)	A	ASTM D695
	37 (5.3)	25 (3.7)	29 (5.3)	21 (3.1)	Y			
	54 (7.8)	37 (5.3)	52 (7.5)	43 (6.3)	Z			
ultimate strain	4.0	4.3	8.5	8.4	X	%	A	ASTM D695
	3.3	3.3	7.7	7.8	Y			
	8.7	8.5	12.5	17.6	Z			
Moisture Absorption	0.02		0.02		N/A	%	.062" (1.6mm) D48/50	ASTM D570
Thermal Conductivity	0.22		0.20		Z	W/m/K	80°C	ASTM C518
Coefficient of Thermal Expansion	22		31		X	ppm/°C	0-100°C	IPC-TM-650, 2.4.41
	28		48		Y			
	173		237		Z			
Td	500		500		N/A	°C TGA	N/A	ASTM D3850
Density	2.2		2.2		N/A	gm/cm ³	N/A	ASTM D792
Copper Peel	27.2 (4.8)		31.2 (5.5)		N/A	pli (N/mm)	1 oz (35mm) EBC foil after solder float	IPC-TM-650 2.4.8
Flammability	V-0		V-0		N/A	N/A	N/A	UL94
Lead-Free Process Compatible	Yes		Yes		N/A	N/A	N/A	N/A

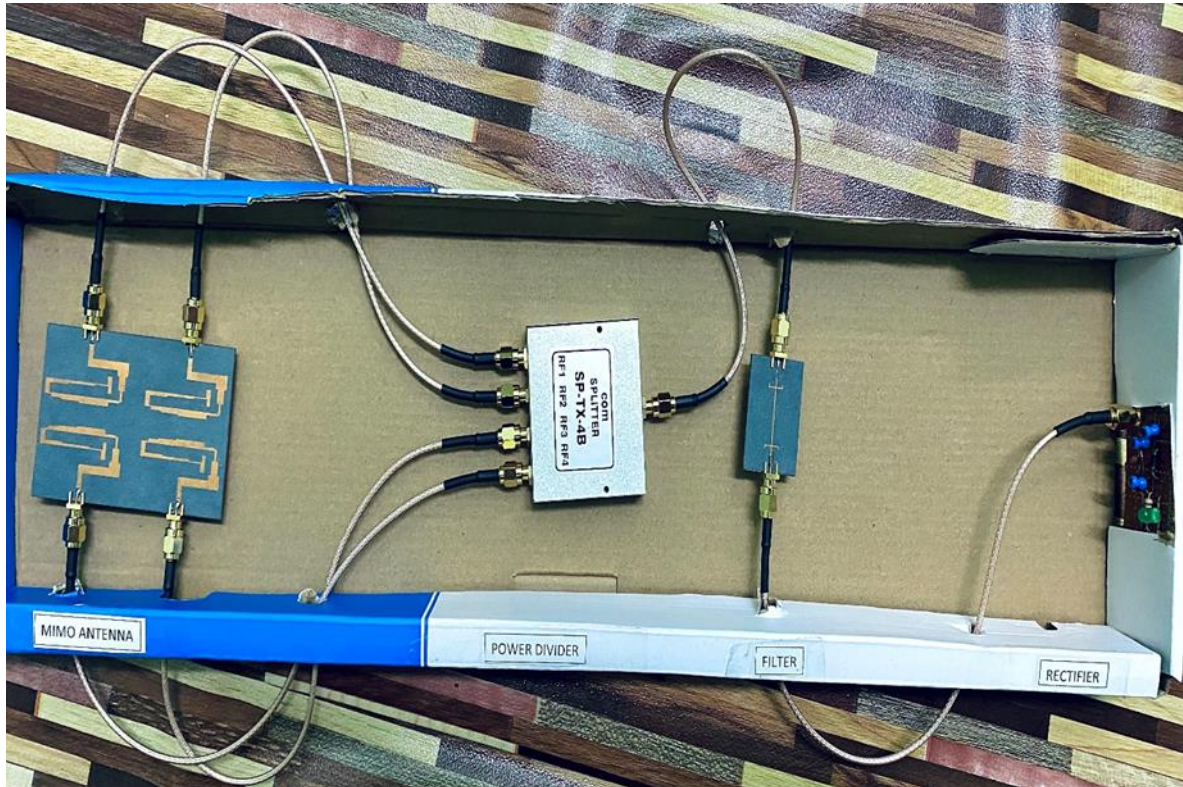
APPENDIX B

The fabricated filter.



APPENDIX C

Prototype of the integrated device.



APPENDIX D


Photo of group member.

(From left: Abdul Wafiy, Muhammad Izzuddin, Muhammad Hafizuddin.)



APPENDIX E

Presentation poster.



G14

WIDEBAND MIMO ANTENNA DEVELOPMENT FOR WIRELESS COMMUNICATION

Supervisor: Dr. Mohammed Nazmus Shakib
 Students: Muhammad Izzuddin bin Jauri (TB17137)
 Abdul Wafiy bin Kassim (TB17060)
 Muhammad Hafizuddin bin Izran (TB17139)

FTKEE

PRODUCT BACKGROUND

Multiple Input Multiple Output (MIMO) antenna is a communication system technology for future 5g and onwards, design antenna operating in 2.4GHz and New frequency Sub-6GHz with microstrip line. The RF energy will convert to DC by design prototype Rectifier that can make wireless system.

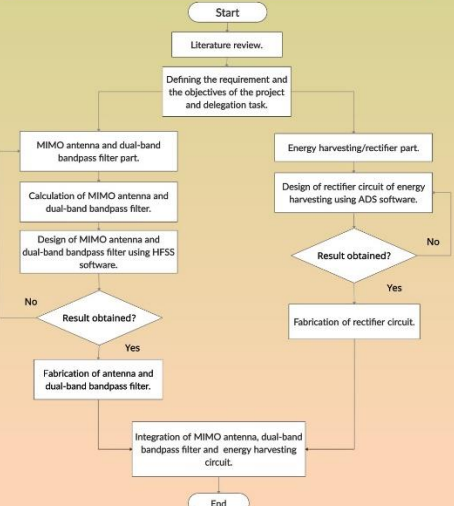
OBJECTIVE

- To design MIMO antenna for wireless connection.
- To develop and simulate MIMO integrated filter to wireless communication. The band are 2.4GHz (WLAN) and 3.5GHz - 4.2GHz (5G Sub-6GHz NR frequency bands)
- To evaluate integrated device for energy harvesting purpose.

BENEFIT

- Low cost, compact size and light weight.
- Can use in rural area.

METHODOLOGY/MATERIALS



SYSTEM MECHANISM

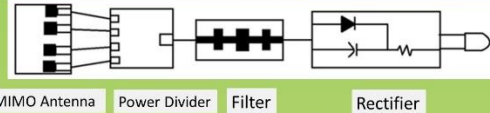


Figure 1: Block diagram of the system.

RESULT & DISCUSSION

MIMO Antenna

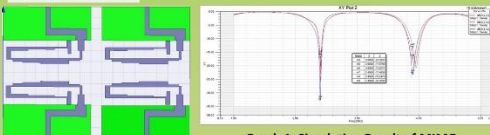


Figure 2: Design of MIMO antenna
Graph 1: Simulation Result of MIMO antenna

Filter

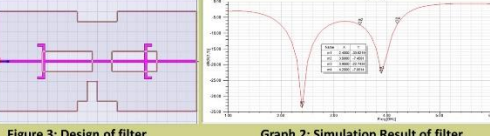


Figure 3: Design of filter.
Graph 2: Simulation Result of filter.

Energy Harvesting

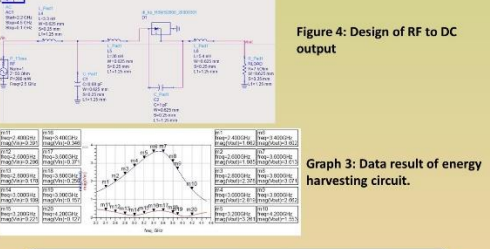



Figure 4: Design of RF to DC output
Figure 3: Data result of energy harvesting circuit.

MARKETIBILITY

- Attract to the telecommunication company such as Telekom Malaysia, Maxis, Celcom and others.
- Demand from the global market because compactness in device system for the great future.

Project Leader: Dr. Mohammed Nazmus Shakib
 Contact Info.: 016-3571283
 nazmus@ump.edu.my



FUNDING ACKNOWLEDGEMENT
 This project was supported by FTKEE under Senior Design Project (SDP) 2021.